FLUIDIZED BED CONVERSION CONFERENCE 2022
8-11th May 2022, Chalmers University of Technology (Sweden)

Solid Flux Measurement in Chemical Looping Gasification Based on Solid Samples

Falko Marx[1], Paul Dieringer[1], Jochen Ströhle[1], Bernd Epple[1]

[1] *Institute for Energy Systems & Technology, Technische Universität Darmstadt, Otto-Berndt-Str. 2, 64287 Darmstadt, Germany;*

Corresponding Author: Falko Marx, falko.marx@est.tu-darmstadt.de

Abstract

Chemical looping gasification is a novel dual fluidized bed technology for the conversion of solid feedstock to a nitrogen-free syngas without the need of pure oxygen. Recently, efforts have been made to advance chemical looping gasification towards autothermal operation. For autothermal operation, the solids flux between the two reactors becomes important, as it transports the required sensible heat in addition to the oxygen required for the process. As no reliable method exists to accurately measure the solids flux under process conditions without extensive calibration under such conditions, a method has been devised utilizing the process specifics of chemical looping gasification to allow for calibration of online measurement equipment without opening the reactor system. This method utilizes solid samples from coupling elements to calculate the solids flux with an overall uncertainty of +/- 15%.

Keywords: Chemical looping gasification, solids flow measurement, fluidized bed.

1 Introduction

Spurred by the increasing pace of climate change, research in carbon neutral and carbon negative processes has increased in order to combat the global warming. One focus is the decarbonisation of the transport sector. While for road transport electrification is a viable option, aviation and maritime transport require different approaches. Here, the production of bio-fuels using the well-known Fischer-Tropsch process is one such option. However, thermal conversion of biomass into the required syngas for the synthesis step is still not commercialized. One process offering the possibility of virtually no CO_2 emissions, when combined with a suitable separation step during gas cleaning, is the chemical looping gasification (CLG), which has seen increasing research activity into scale up. It utilizes a metal oxide powder, which is cyclical oxidized and reduced while being transported back and forth between two fluidized bed reactors, to supply oxygen to the gasification process without the need for an expensive air separation unit.

CLG has been successfully demonstrated in lab scale [1]–[7] and advances towards autothermal operation are being made [8]–[10]. These advances stress the importance of the oxygen carrier (OC) not only for the transport of oxygen, but also for the transport of sensible heat from fuel reactor (FR) to air reactor (AR) as high heating demands inside the FR cannot be compensated by external electrical reactor heating for successful process deployment. However, reliable measurements of the solids circulation are difficult to obtain. Moreover, the solids transported from the FR towards the AR consist not only of the reduced OC material, but include also a fraction of unconverted feedstock in the form of fixed carbon, called carbon slip, and ash. Methods to obtain quantitative data for the OC circulation between the reactors can be classified as online, offline, invasive and non-invasive [11] additionally simulation and cold-flow studies can be used to generate the data afterwards. Nonetheless, for elaborate and expensive experiments as described in [9] the measurement of solid circulation during the experiments and from material samples results in far more convincing data than a posteriori

generated data from cold flow models or simulation. This study proposes a new method utilizing solid samples taken from coupling elements during experimental operation to calculate the solids flux.

2 State of the Art in Measurement of Solid Circulation

2.1 Online Measurement

Stollhof et al. [12] investigated methods to estimate the solid circulation rate based on the amount of fluidization medium, particle properties and pressure profile in the reactors which can be applied to the hot reactor system. However, a reported deviation of $\pm$ 40 % is discouraging as such deviations in solid circulation could potentially result in a FR temperature drop of more than 150°C [8] negatively impacting conversion and syngas quality. Direct measurement using impact force of the particle flow is limited by the maximum permissible temperature of the measurement equipment and can therefore not be used under process conditions.

Online Measurements using optical sensing have been successfully tested in cold flow configurations [13] and in 2D setups [14]. However, the application to large-scale units operating at high temperatures is not possible as the sensor cannot measure deep inside the solid flux or through the refractory lined reactor walls. Other setups using moving mechanical equipment inside the solid stream [15] seem problematic with regards to the lifetime under the harsh process conditions.

Direct online measurement using the microwave and Doppler effect is an option, but usually requires extensive calibration under process conditions, which are not feasible, as the loop has to be broken for calibration. It can be calibrated under cold conditions, but the influence of the temperature cannot be reliably compensated as no data is available yet.

Using tracer particles as described in [11] is likely to be of limited use, as the continuous removal of agglomerates poses the possibility of the removal of the tracer particle.

2.2 Offline Measurement

Solid circulation can be determined via scaling laws based on measurement in a cold flow model with measurements inside the coupling elements (e.g. loop seals) or with another method. The existing scaling according to the simplified set from Glicksmann [16] shows deviation from a perfectly scaled model (Table 1). A perfectly scaled cold flow model is difficult to realize for metal powders, as the cold flow model would need to be filled with Helium or use radioactive materials. Not perfectly scaled cold flow models can give a quantitative measurement in the right order of magnitude, but the exact error created cannot be assessed.

Table 1: Scaling of a Cold Flow Model for the experimental facility described in [9]. AR: air reactor, FR: fuel reactor

Dimensionless Term	AR_{Pilot}	AR_{Modell}	FR_{Pilot}	FR_{Modell}	$\frac{AR_{Pilot}}{AR_{Modell}}$	$\frac{FR_{Pilot}}{FR_{Modell}}$
$\frac{\bar{d}_m\ \rho_g\ u_0}{\mu}$	2,81	6,07	4,57	11,09	0,46	0,41
$\frac{u_0^2}{g\ D_R}$	2,2	2,2	10,85	10,85	1	1
$\frac{\rho_s}{\rho_g}$	16615	8327	21362	8327	1,99	2,57
$\frac{D_R}{\bar{d}_m}$	3831	3748	2597	2534	1,02	1,02
$\frac{G_s}{\rho_s\ u_0}$	$4{,}56 \cdot 10^{-4}$	$4{,}76 \cdot 10^{-4}$	$5{,}66 \cdot 10^{-4}$	$5{,}66 \cdot 10^{-4}$	0,96	1

Calculations using CFD require validation of the model to allow for an assessment of the quality of the generated data. However, during endeavours of upscaling such models extrapolate far outside their validation range, as the data to be obtained is the data required for validation. Theoretically, the solid circulation is obtainable via the heat balance. However, accurate knowledge of heat losses through the refractory lined reactor walls under changing ambient conditions is challenging.

Using offline solid samples from the coupling elements and the specifics of the CLG process is the only option to obtain the solid circulation with moderate effort and expenditures while yielding good accuracy. Moreover, the error can be quantified by the calculation of the propagated uncertainties. The underlying calculation and required measurements are presented here in detail.

3 New Method for Determining the Solid Circulation from Offline Samples

A simplified flow sheet of the 1 MW_{th} experimental facility for autothermal operation of the CLG process is shown in Figure 1 and described in detail elsewhere [9]. It shows the reactor system including the relevant measurement sites and sampling points in the installed loop seals for this Method. As AR operation in sub-stoichiometric conditions has advantages [8]–[10], it can be assumed that all oxygen in the air flow fed to the AR is consumed.

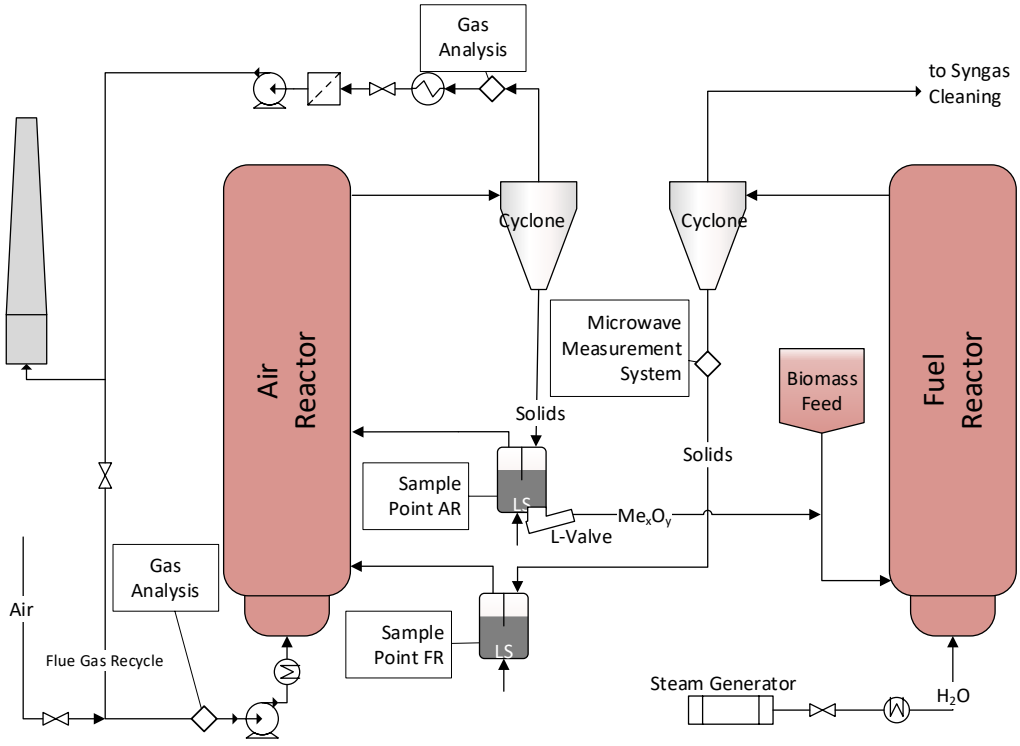

Figure 1: Schematic of the chemical looping gasification process indicating relevant measurement sites and sample position

Assuming steady-state operation of the process, the basis for the calculation is the oxygen supplied to the fuel reactor (FR):

$$\dot{m}_{ox} = y_{ox} \cdot \dot{m}_{AR,in}$$

Where y_{ox} is the mass fraction of oxygen in the fluidization media, and $\dot{m}_{AR,in}$ is the amount of fluidization medium supplied to the AR measured by gas analysis and venturi tube or orifice plate. However, if the conversion of oxygen is incomplete or carbon slip from the FR is significant, the analysis of the AR flue gas can be used to compensate for this effects, and the amount of oxygen supplied towards the FR is:

$$\dot{m}_{ox} = y_{ox,in} \cdot \dot{m}_{AR,in} - \left(y_{ox,out} + y_{CO2} \cdot {}^{32}/_{44}\right)\dot{m}_{AR,out}$$

requiring gas analysis and flow measurement. As no oxidation or reduction reactions occur inside the loop seals, samples of the circulating oxygen carrier taken in the coupling elements can be considered representative for the reactor outlet. With knowledge of the oxygen carrying capacity R_{oc} and the oxidation degree $X_s$of the sample as defined by [17]:

$$X_s = \frac{m_{oc,LS} - m_{oc,red}}{R_{oc} \cdot m_{oc,ox}}$$

$$R_{oc} = \frac{m_{oc,ox} - m_{oc,red}}{m_{oc,ox}}$$

calculation of the solids flux becomes possible as it defines a ratio of oxygen and OC material.

3.1 Analysis of Oxygen Content in Loop Seal Samples.

The oxygen carrying capacity is an important parameter of the oxygen carrier. It is subject to change during plant operation due to deactivation of OC material and accumulation of ash inside the system. The determination of R_{oc} requires oxidation and reduction of a sample usually done in TGA experiments (e.g. [18]). However, knowledge of the exact value of the oxygen carrying capacity R_{oc} is not required for this method. The samples can be analysed regarding oxygen content using commonly available lab equipment by simple oxidation with air. The sample from the FR outlet gives a relative mass increase $z_{ox,FR}$ during oxidation:

$$z_{ox,FR} = \frac{m_{O2,FR}}{m_{e,FR}} = \frac{m_{e,FR} - m_{s,FR}}{m_{e,FR}}$$

With the mass after full oxidation of the sample m_e and the mass before oxidation m_s. The same analysis for the AR outlet gives

$$z_{ox,AR} = \frac{m_{O2,AR}}{m_{e,AR}} = \frac{m_{e,AR} - m_{s,AR}}{m_{e,AR}} = \frac{m_{e,AR} - (m_{oc} + m_O)}{m_{e,AR}}$$

Where $m_{s,AR}$ consists of the mass of the oxygen carrier, m_{oc}, and the mass of the oxygen uptake from the AR, m_O. The difference in relative mass change of two samples from the same operational state must be the oxygen transported towards the FR.

$$z_{ox,FR} - z_{ox,AR} = \frac{m_{e,FR} - m_{s,FR}}{m_{e,FR}} - \frac{m_{e,AR} - m_{oc,AR}}{m_{e,AR}} + \frac{m_O}{m_{e,AR}}$$

In both streams, the OC mass must be the same, so the first two terms on the right side cancel out and it remains

$$z_{ox,FR} - z_{ox,AR} = \frac{m_O}{m_{e,AR}} = z_o$$

However, as the samples are normalized using the mass after oxidation, which is not a state of the process stream, it has to be converted to:

$$x_o = \frac{{}^{m_O}/_{m_{e,AR}}}{{}^{m_{s,AR}}/_{m_{e,AR}}} = \frac{\frac{m_{e,FR} - m_{s,FR}}{m_{e,FR}} - \frac{m_{e,AR} - m_{s,AR}}{m_{e,AR}}}{{}^{m_{s,AR}}/_{m_{e,AR}}}$$

3.2 Consideration of Carbon Slip

Assuming the presence of significant carbon slip, the mass loss of carbon oxidation must be accounted for in the sample from the FR outlet

$$m_{s,FR} = m_{oc,FR} + m_c$$

necessitating the analysis of the carbon content m_c, which can be analysed from the sample using standard lab techniques for ultimate analysis. The AR outlet solid sample does not need compensation for carbon content, as carbon oxidation is favoured over OC oxidation [18]–[20]. When a nitrogen recycle is used to control the oxygen input as described by Dieringer et al. [8], the input to the reactor contains a fraction of CO_2 as well and a correction must be applied. The resulting solids flux towards the FR is then calculated to:

$$\dot{m}_{solids} = \frac{\dot{m}_{ox}}{x_o} = \frac{y_{ox,in} \cdot \dot{m}_{AR,in} - y_{ox,out} \cdot \dot{m}_{AR,out} - {}^{32}/_{44} \left(y_{CO2,\mathrm{out}} \cdot \dot{m}_{AR,out} - y_{CO2,\mathrm{in}} \cdot \dot{m}_{AR,in} \right)}{\frac{\frac{m_{e,FR} - m_{s,FR} - m_c}{m_{e,FR}} - \frac{m_{e,AR} - m_{s,AR}}{m_{e,AR}}}{{m_{s,AR}}/{m_{e,AR}}}}$$

$$= \frac{\left(y_{ox,in} + {}^{32}/_{44}\, y_{CO2,\mathrm{in}}\right) \cdot \dot{m}_{AR,in} - \left(y_{ox,out} + y_{CO2} \cdot {}^{32}/_{44}\right) \dot{m}_{AR,out}}{\left(\frac{m_{e,FR} - m_{s,FR} - m_c}{m_{e,FR}} - \frac{m_{e,AR} - m_{s,AR}}{m_{e,AR}}\right) \cdot \frac{m_{e,AR}}{m_{s,AR}}}$$

$$= \left[\left(y_{ox,in} + {}^{32}/_{44}\, y_{CO2,\mathrm{in}}\right) \cdot \dot{m}_{AR,in} - \left(y_{ox,out} + y_{CO2} \cdot {}^{32}/_{44}\right) \dot{m}_{AR,out}\right]$$

$$\cdot \left(\frac{m_{e,FR} - m_{s,FR} - m_c}{m_{e,FR}} - \frac{m_{e,AR} - m_{s,AR}}{m_{e,AR}}\right)^{-1} \cdot \frac{m_{s,AR}}{m_{e,AR}}$$

The solid-solid reaction of OC and char inside the loop seals is not considered here. Although Chen et al. [18] show that a solid-solid reaction can occur at the conditions inside the loop seals, the OC leaving the FR is already highly reduced, and the low amount of fixed carbon in the feedstock [9] leads to mass fractions of less than 0.5% carbon inside the loop seal. Moreover, the mean residence time inside the loop seal is less than a minute making the effect negligible.

3.3 Propagation of Uncertainties

Based on case HT2 from [9] (selected here because it yields the best feedstock conversion and thus the lowest carbon slip) and the assumption that half of the fixed carbon from the feedstock is transported towards the AR the propagation of uncertainties has been estimated using the values from Table 2. The partial derivatives are given in the appendix. The relative uncertainty is about 15 % giving a good estimation of the solids flux considering the low cost solution used.

Table 2: Values used for the estimation of the uncertainty (partially from [9])

	Value	Uncertainty	Unit
$\dot{m}_{AR,in}$	1142	30	kg/h
$\dot{m}_{AR,out}$	1062	30	kg/h
$y_{ox,in}$	0,15	0,009	
$y_{CO2,\mathrm{in}}$	0,025	0,009	
$y_{ox,out}$	0	0,009	
$y_{CO2,\mathrm{out}}$	0,09	0,009	
$m_{s,FR}$	0,010000	1E-10	kg
$m_{e,FR}$	0,011000	1E-10	kg
m_c	0,000015	1E-10	kg
$m_{s,AR}$	0,010000	1E-10	kg
$m_{e,AR}$	0,010845	1E-10	kg
$\dot{m}_{solids}$	9827	1449	kg/h

4 Conclusion

The measurement of solid flux in a closed loop system of circulating fluidized bed reactors remains a challenge. Although measurement techniques for the online measurement exist, they are either not applicable in high temperatures or require extensive calibration under operating conditions. As the opening of the loop is not possible under process conditions, an alternative method using the specifics of the CLG process and solid samples has been devised. The relative uncertainty of about 15% is much smaller than the uncertainties of other methods correlating pressure profiles.

Although this method is an offline method, it can be used to calibrate online measurement equipment based on the Doppler effect which is installed in the pilot plant to obtain much more data points based on recorded raw values. The uncertainty of the microwave measurement is much smaller than the uncertainty of the presented method, so it is assumed that the overall uncertainty is the uncertainty of the presented method. The application of this method to the calibration of the online microwave measurement system installed in the pilot plant allows for the reliable measurement of the solids circulation during upcoming experiments.

Acknowledgements: The authors gratefully acknowledge the financial support of the European Union's Horizon 2020—Research and Innovation Framework Programme under grant agreement No. 817841 (Chemical Looping gasification foR sustainAble production of biofuels—CLARA).

References

[1] O. Condori, F. García-Labiano, L. F. de Diego, M. T. Izquierdo, A. Abad, and J. Adánez, 'Biomass chemical looping gasification for syngas production using ilmenite as oxygen carrier in a 1.5 kWth unit', *Chem. Eng. J.*, vol. 405, p. 126679, Feb. 2021, doi: 10.1016/j.cej.2020.126679.

[2] S. Huseyin, G. Wei, H. Li, F. He, and Z. Huang, 'Chemical-looping gasification of biomass in a 10 kWth interconnected fluidized bed reactor using Fe2O3/Al2O3 oxygen carrier', *J. Fuel Chem. Technol.*, vol. 42, no. 8, pp. 922–931, Aug. 2014, doi: 10.1016/S1872-5813(14)60039-6.

[3] Q. Guo, Y. Cheng, Y. Liu, W. Jia, and H.-J. Ryu, 'Coal Chemical Looping Gasification for Syngas Generation Using an Iron-Based Oxygen Carrier', *Ind. Eng. Chem. Res.*, vol. 53, no. 1, pp. 78–86, Jan. 2014, doi: 10.1021/ie401568x.

[4] G. Wei, F. He, Z. Huang, A. Zheng, K. Zhao, and H. Li, 'Continuous Operation of a 10 kW $_{th}$ Chemical Looping Integrated Fluidized Bed Reactor for Gasifying Biomass Using an Iron-Based Oxygen Carrier', *Energy Fuels*, vol. 29, no. 1, pp. 233–241, Jan. 2015, doi: 10.1021/ef5021457.

[5] I. Samprón, L. F. de Diego, F. García-Labiano, M. T. Izquierdo, A. Abad, and J. Adánez, 'Biomass Chemical Looping Gasification of pine wood using a synthetic Fe2O3/Al2O3 oxygen carrier in a continuous unit', *Bioresour. Technol.*, vol. 316, p. 123908, Nov. 2020, doi: 10.1016/j.biortech.2020.123908.

[6] H. Ge, W. Guo, L. Shen, T. Song, and J. Xiao, 'Experimental investigation on biomass gasification using chemical looping in a batch reactor and a continuous dual reactor', *Chem. Eng. J.*, vol. 286, pp. 689–700, Feb. 2016, doi: 10.1016/j.cej.2015.11.008.

[7] H. Ge, W. Guo, L. Shen, T. Song, and J. Xiao, 'Biomass gasification using chemical looping in a 25 kW th reactor with natural hematite as oxygen carrier', *Chem. Eng. J.*, vol. 286, pp. 174–183, Feb. 2016, doi: 10.1016/j.cej.2015.10.092.

[8] P. Dieringer, F. Marx, F. Alobaid, J. Ströhle, and B. Epple, 'Process Control Strategies in Chemical Looping Gasification—A Novel Process for the Production of Biofuels Allowing for Net Negative CO2 Emissions', *Appl. Sci.*, vol. 10, no. 12, p. 26, Jun. 2020, doi: 10.3390/app10124271.

[9] F. Marx, P. Dieringer, J. Ströhle, and B. Epple, 'Design of a 1 MWth Pilot Plant for Chemical Looping Gasification of Biogenic Residues', *Energies*, vol. 14, no. 9, p. 2581, Apr. 2021, doi: 10.3390/en14092581.

[10] I. Samprón, L. F. de Diego, F. García-Labiano, and M. T. Izquierdo, 'Optimization of synthesis gas production in the biomass chemical looping gasification process operating under auto-thermal conditions', *Energy*, vol. 226, p. 120317, Jul. 2021, doi: 10.1016/j.energy.2021.120317.

[11] S. Bhusarapu, P. Fongarland, M. H. Al-Dahhan, and M. P. Duduković, 'Measurement of overall solids mass flux in a gas–solid Circulating Fluidized Bed', *Powder Technol.*, vol. 148, no. 2–3, pp. 158–171, Nov. 2004, doi: 10.1016/j.powtec.2004.09.007.

[12] M. Stollhof, S. Penthor, K. Mayer, and H. Hofbauer, 'Estimation of the solid circulation rate in circulating fluidized bed systems', *Powder Technol.*, vol. 336, pp. 1–11, Aug. 2018, doi: 10.1016/j.powtec.2018.05.033.
[13] S. Matsuda, 'Measurement of solid circulation rate in a circulating fluidized bed', *Powder Technol.*, vol. 187, no. 2, pp. 200–204, Oct. 2008, doi: 10.1016/j.powtec.2008.02.004.
[14] J. A. Medrano, M. Nordio, G. Manzolini, M. van Sint Annaland, and F. Gallucci, 'On the measurement of solids circulation rates in interconnected fluidized beds: Comparison of different experimental techniques', *Powder Technol.*, vol. 302, pp. 81–89, Nov. 2016, doi: 10.1016/j.powtec.2016.08.035.
[15] J. C. Ludlow, E. R. Monazam, and L. J. Shadle, 'Improvement of continuous solid circulation rate measurement in a cold flow circulating fluidized bed', *Powder Technol.*, vol. 182, no. 3, pp. 379–387, Mar. 2008, doi: 10.1016/j.powtec.2007.06.031.
[16] L. R. Glicksman, M. Hyre, and K. Woloshun, 'Simplified scaling relationships for fluidized beds', *Powder Technol.*, vol. 77, no. 2, pp. 177–199, Nov. 1993, doi: 10.1016/0032-5910(93)80055-F.
[17] A. Larsson, M. Israelsson, F. Lind, M. Seemann, and H. Thunman, 'Using Ilmenite To Reduce the Tar Yield in a Dual Fluidized Bed Gasification System', *Energy Fuels*, vol. 28, no. 4, pp. 2632–2644, Apr. 2014, doi: 10.1021/ef500132p.
[18] A. Cuadrat, A. Abad, F. García-Labiano, P. Gayán, L. F. de Diego, and J. Adánez, 'The use of ilmenite as oxygen-carrier in a 500Wth Chemical-Looping Coal Combustion unit', *Int. J. Greenh. Gas Control*, vol. 5, no. 6, pp. 1630–1642, Nov. 2011, doi: 10.1016/j.ijggc.2011.09.010.
[19] L. Chen, 'The direct solid-solid reaction between coal char and iron-based oxygen carrier and its contribution to solid-fueled chemical looping combustion', *Appl. Energy*, p. 10, 2016, doi: 10.1016/j.apenergy.2016.09.085.
[20] H. Leion, T. Mattisson, and A. Lyngfelt, 'Solid fuels in chemical-looping combustion', *Int. J. Greenh. Gas Control*, vol. 2, no. 2, pp. 180–193, Apr. 2008, doi: 10.1016/S1750-5836(07)00117-X.
[21] Q. Song *et al.*, 'Chemical-looping combustion of methane with CaSO4 oxygen carrier in a fixed bed reactor', *Energy Convers. Manag.*, vol. 49, no. 11, pp. 3178–3187, Nov. 2008, doi: 10.1016/j.enconman.2008.05.020.

Abbreviations

AR	Air reactor
FR	Fuel reactor
OC	Oxygen carrier

Symbols

m	Mass	kg
$y_{ox,in}$	Mass fraction	

Subscripts

in	input towards reactor
out	output of reactor
s	state at start of measurement / initial weight
e	state at end of measurement / resulting weight
c	carbon
o	oxygen

Appendix: Propagation of Uncertainties: Partial Derivatives

$$\dot{m}_{solids} = \left[\left(y_{ox,in} + {}^{32}/_{44}\, y_{CO2,\mathrm{in}}\right) \cdot \dot{\mathrm{m}}_{AR,in} - \left(y_{ox,out} + y_{CO2} \cdot {}^{32}/_{44}\right)\dot{\mathrm{m}}_{AR,out}\right] \cdot \left(\frac{m_{e,FR} - m_{s,FR} - m_c}{m_{e,FR}} - \frac{m_{e,AR} - m_{s,AR}}{m_{e,AR}}\right)^{-1} \cdot \frac{m_{s,AR}}{m_{e,AR}} = A \cdot B^{-1} \cdot C$$

$$A = \left[\left(y_{ox,in} + {}^{32}/_{44}\, y_{CO2,\mathrm{in}}\right) \cdot \dot{\mathrm{m}}_{AR,in} - \left(y_{ox,out} + y_{CO2} \cdot {}^{32}/_{44}\right)\dot{\mathrm{m}}_{AR,out}\right]$$

$$B = \left(\frac{m_{e,FR} - m_{s,FR} - m_c}{m_{e,FR}} - \frac{m_{e,AR} - m_{s,AR}}{m_{e,AR}}\right)$$

$$C = \frac{m_{s,AR}}{m_{e,AR}}$$

$$\frac{\partial \dot{m}_{solids}}{\partial y_{ox,in}} = \dot{\mathrm{m}}_{AR,in} \cdot B^{-1} \cdot C$$

$$\frac{\partial \dot{m}_{solids}}{\partial y_{CO2,in}} = \frac{32}{44} \cdot \dot{\mathrm{m}}_{AR,in} \cdot B^{-1} \cdot C$$

$$\frac{\partial \dot{m}_{solids}}{\partial \dot{\mathrm{m}}_{AR,in}} = \left(y_{ox,in} + {}^{32}/_{44}\, y_{CO2,\mathrm{in}}\right) \cdot B^{-1} \cdot C$$

$$\frac{\partial \dot{m}_{solids}}{\partial y_{ox,out}} = -\dot{\mathrm{m}}_{AR,out} \cdot B^{-1} \cdot C$$

$$\frac{\partial \dot{m}_{solids}}{\partial y_{CO2,out}} = -\frac{32}{44} \cdot \dot{\mathrm{m}}_{AR,out} \cdot B^{-1} \cdot C$$

$$\frac{\partial \dot{m}_{solids}}{\partial \dot{\mathrm{m}}_{AR,out}} = -\left(y_{ox,out} + {}^{32}/_{44}\, y_{CO2,\mathrm{out}}\right) \cdot B^{-1} \cdot C$$

$$\frac{\partial \dot{m}_{solids}}{\partial m_{e,FR}} = A \cdot (-1) \cdot B^{-2} \cdot \left(\frac{-m_{s,FR} - m_c}{-m_{e,FR}^2}\right) \cdot C$$

$$\frac{\partial \dot{m}_{solids}}{\partial m_{s,FR}} = A \cdot (-1) \cdot B^{-2} \cdot \left(\frac{-1}{m_{e,FR}}\right) \cdot C$$

$$\frac{\partial \dot{m}_{solids}}{\partial m_c} = A \cdot (-1) \cdot B^{-2} \cdot \left(\frac{-1}{m_{e,FR}}\right) \cdot C$$

$$\frac{\partial \dot{m}_{solids}}{\partial m_{e,AR}} = A \cdot (-1) \cdot B^{-2} \cdot \left(\frac{m_{s,AR}}{-m_{e,AR}^2}\right) \cdot C + A \cdot B^{-1} \cdot \frac{m_{s,AR}}{-m_{e,AR}^2}$$

$$\frac{\partial \dot{m}_{solids}}{\partial m_{s,AR}} = A \cdot (-1) \cdot B^{-2} \cdot \left(\frac{-1}{-m_{e,AR}}\right) \cdot C + A \cdot B^{-1} \cdot \frac{1}{m_{e,AR}}$$